The 2015 World Congress on
Advances in Structural Engineering and Mechanics (ASEM15)
Incheon, Korea, August 25-29, 2015

Detection of tensile force relaxation through eddy current measurement of a pre-stressing strand

Ji-Min Kim[1)], Jun Lee[2)] and *Hoon Sohn[3)]

[1), 2), 3)] *Department of Civil Engineering, KAIST, Daejeon 350-701, Korea*
[1)] jimin.kim@kaist.ac.kr; [2)] leejun@kaist.ac.kr; [3)] hoonsohn@kaist.ac.kr

ABSTRACT

A new monitoring technique to inspect the force relaxation of a pre-stressing strand is developed based on the eddy current measurement. The advantages of the proposed technique are: (1) low cost, (2) low power consumption, (3) simple installation and (4) robustness of sensor healthiness. A specially designed cylinder-type eddy current sensor is mounted on the exposed surface of a wedge holding a strand under the premise that the variation of the pre-stressing strand force also alters the stress level on the exposed surface of the wedge. The proposed tensile force inspection system is experimentally validated by taking measurements from a 3.3 m long and Φ 15.2 mm pre-stressing strand. As tensile force decreases from 180 kN to 30 kN gradually, a monotonic relationship between the tensile force and the proposed damage index is successfully observed.

1. INTRODUCTION

Pre-stressing using a pre-stressing strand is a common practice to offset the tensile force induced by the self-weight of a concrete structure. Its cost-effective feature makes builders to employ pre-stressing method. As the concrete structure is under service, however, the tensile force of the pre-stressing strand is gradually lost. The reason of losing force can be classified as (1) immediate loss due to elastic shortening and frictions at the interface between a strand and a grouting material, and (2) time-dependent loss by steel relaxation and concrete creep. It can compromise the integrity of the entire concrete structure and result in a catastrophic failure of the system. Thus, tensile force inspection is highly required during a life-span of the structure. (Tadros 2003 and Hewson 2008)

In order to effectively inspect the tensile force of a pre-stressing strand, various techniques have been proposed. However, their excessive power consumption and

---

[1)] Graduate student
[2)] Graduate student
[3)] Professor

troublesome installation on extremely narrow inner space of a structure easily brings about sensor damage and highly restrict practicality of the technique under in-situ conditions. For example, electromagnetic sensor requires excessive power to sufficiently magnetize a target pre-stressing strand so that satisfactory performance can be assured (Wang 2006 and Duan 2012) and, an ultrasonic technique requires careful attachment of ultrasonic wave generating piezo-electric sensors to the surface of a strand which is vulnerable to a damage during construction procedures by inevitable contact with adjacent strands (Bartoli 2011). In recent, a specially designed pre-stressing strand is developed which contains an optical fiber with several fiber bragg grating (FBG) sensors at a core wire of the strand (Kim 2012 and Lan 2014). This technique is quite innovative in that tensile force information at each FBG sensor along axial direction of the pre-stressing strand can be obtained. However, the insertion of an optical fiber to a pre-stressing strand should be conducted before construction in factory, thereby manufacturing expenses including a long optical fiber and FBG sensors considerably rise. On the other hand, a tensile force inspection technique using eddy current sensor (ECS) was proposed so that the required power consumption and costs can be significantly reduced (Schoenekess 2007). Nevertheless, the location of ECS installation has been a bottleneck to be employed in in-situ environments. ECS should be closely contact on outer surface of a target pre-stressing strand to directly measure the electromagnetic variation of the strand. Therefore, again, the ECS easily becomes damaged and disabled during the insertion of a bundle of strands into a narrow duct or high-pressure cement grouting process.

In this study, a new inspection technique through eddy current measurement is proposed to detect the tensile force relaxation of a pre-stressing strand. The proposed technique shows following obvious uniqueness: (1) low cost, (2) low power consumption, (3) simple installation without disturbing construction process and (4) robustness of sensor healthiness. The proposed technique detects variations of the generated eddy current on the exposed surface of a wedge using ECS and, present status of a strand force is evaluated by comparing it with a baseline data previously accumulated under an initial condition which represents a tensile force right after the end of pre-stressing. The purposes of this study are as follows: (1) investigation of the relationship between a tensile force and an eddy current on a wedge surface and, (2) development of eddy current based tensile force inspection (EC-TFI) system and its performance validation through a lab-scale experiment.

Section 2 introduces an eddy current testing (ECT) for stress evaluation and proposes an EC-TFI technique with a detailed explanation of its working principles. The EC-TFI system is developed in Section 3 and its experimental validations are provided in Section 4. Brief summary and future works are mentioned in Section 5.

2. EDDY CURRENT BASED TENSILE FORCE INSPECTION (EC-TFI) OF A PRE-STRESSING STRAND

In this section, fundamentals of ECT is analytically explained for stress evaluation based on Maxwell's equations. Then, EC-TFI is proposed and its detailed working principle is described through separate steps.

2.1 Introduction to Eddy Current Testing (ECT)

Fig. 1 shows a basic configuration of ECT for stress evaluation of a target structure. ESC composed of a drive coil and a pick-up coil is placed right above the target structure. By applying alternating voltage at the drive coil, eddy current is induced on the surface of the target structure, and the sequentially-induced voltage in the pick-up coil (V_c) is sensed through the pick-up coil. ECT can evaluate stress condition of the target structure by utilizing the fact that V_c is altered when the target structure's stress is changed as shown in Fig. 1.

The fundamental theory of ECT can be analytically explained using Maxwell's equations (Jackson 1998). When an alternating current flows through the drive coil, a primary magnetic field is generated which is alternating with same frequency as well. By Faraday's law, an electric field is induced causing an eddy current on the surface of the target structure.

$$\nabla \times E_t = -\frac{\partial B_p}{\partial t} \tag{1}$$

E_t is an electric field on the target structure and, B_p is a magnetic flux density induced by the primary magnetic field (H_p) around the target structure which can be expressed as follows.

$$B_p = \mu H_p \tag{2}$$

Here, μ denotes a magnetic permeability of the target structure. In sequence, current density of the target structure (J_t) is determined by E_t and its electric resistivity (ρ_t) which can be altered through *piezo-resistive effects*, meaning that a material's electric resistivity depends on the stress condition that it is subjected to.

$$J_t = \frac{1}{\rho_t} E_t \tag{3}$$

$$\nabla \times H_s = J_t + \frac{\partial D}{\partial t} \tag{4}$$

H_s means a secondary magnetic field and D denotes a displacement current. If we assume that the target structure is composed of highly conductive material, D can be ignored. Eq. (4) infers that the magnitude of J_t directly affects the generation of H_s. Then, a current density of the pick-up coil (J_c) is determined as the following equation, which is induced by an alternating magnetic field, i.e. combination of H_p and H_s.

$$J_c = \frac{1}{\rho_c} E_c \tag{5}$$

$$\nabla \times E_c = -\frac{\partial (B_p + B_s)}{\partial t} \tag{6}$$

E_c is an electric field in the pick-up coil. In here, B_p and B_s should be considered together in order to express E_c, because H_p and H_s exist at the same time around the pick-up coil. B_p and B_s mean the magnetic flux density related with H_p and H_s, respectively.

In order to evaluate the stress level of the target structure, ECT directly measures V_c which has a linear relationship with J_c. Let us assume the following specific condition. The intensity of B_p is decided by the pre-determined experimental parameters of an excitation system and, electric resistivity of ECS is supposed as to be fixed during the experiment. Then, the only factor making J_c and V_c varied is the electric resistivity of the target structure differed by its stress condition. That is, the alteration of J_c or V_c can be used as an indicator to detect stress variation of the target structure.

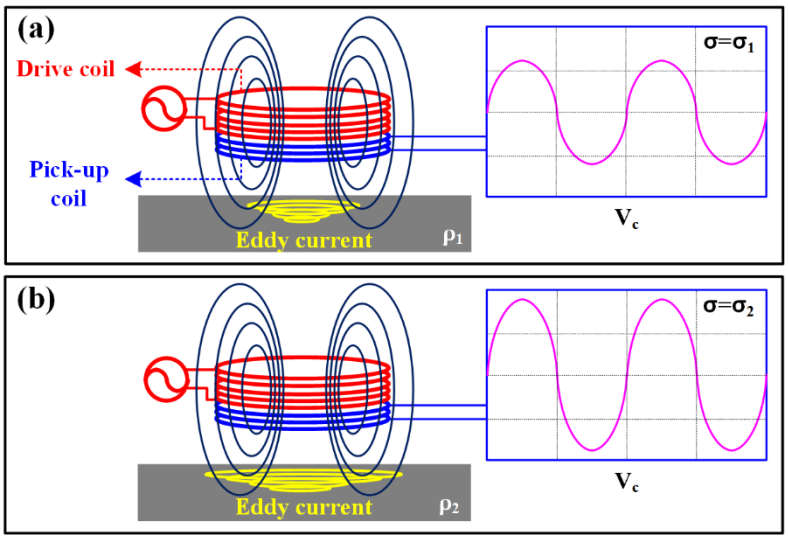

Fig. 1. Basic configuration of ECT to evaluate a target structure subjected to different stress conditions: (a) $\sigma = \sigma_1$, (b) $\sigma = \sigma_2$

2.2 Working Principle of EC-TFI

This section explains working principle of the proposed EC-TFI. EC-TFI is based on the premise that the variation of a pre-stressing strand force also alters the stress level on the exposed surface of a wedge as described in Fig. 2. Before tensile force is applied to the pre-stressing strand, the condition between the pre-stressing strand and the wedge can be considered as a simple contact. Then, as tensile force becomes to be applied gradually, the wedge is tightly fitted into an empty space of an anchor head which is a structural member to distribute the applied stress to a bearing plate. In sequence, a compressive force is provided along to a radial direction of the wedge. According to the *piezo-resistive effects* explained in the previous section, electric resistivity of the wedge is altered from ρ_0 to ρ_1, before and after applying a tensile force to the pre-stressing strand, respectively. Thus, even when an eddy current is induced on the exposed surface of the wedge by exactly same H_p, its current density varies with

the pre-stressing strand force so that the corresponding V_c is altered as well. This premise infers that tensile force of the pre-stressing strand can be inspected by measuring and analyzing V_c. If a system has a baseline data previously acquired in an intact condition, a tensile force relaxation of the pre-stressing strand can be properly detected by comparing the measured data with the baseline data as a reference.

The entire process of tensile force inspection follows the three steps described in Fig. 3: (1) Eddy current generation on a wedge surface by flowing alternating current through a drive coil, (2) Measurement of an electromagnetically induced voltage signal in a pick-up coil and, (3) Tensile force estimation through calculation of the defined damage index (DI). Through these three steps, a strand force inspection and relaxation detection can be successfully carried out by simply attaching an ECS on an outer surface of a wedge. The detailed description for each step is as follows.

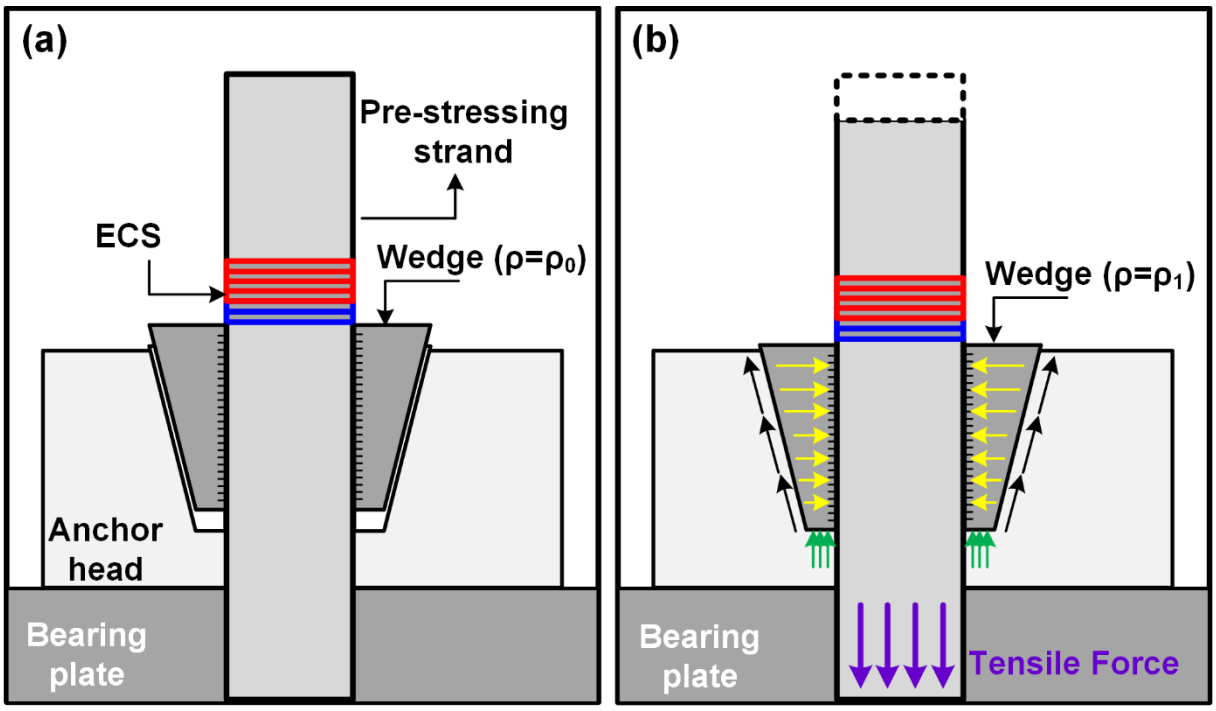

Fig. 2. Stress distribution of the exposed surface of a wedge:
(a) before and (b) after a tensile force is applied to a pre-stresing strand

(1) Eddy current generation on a wedge surface by flowing alternating current through a drive coil:

An ECS is mounted on the exposed surface of a wedge as shown in Fig. 3. Here, a pick-up coil is attached to the wedge surface to sense even small amount of electromagnetic alterations from the wedge surface and, a drive coil is located at the right above it. Then, a chirp signal of the predetermined frequency range and amplitude is generated and applied to the drive coil to induce alternating current as shown in the step (1) in Fig. 3. In consequent, alternating H_p is produced around the drive coil,

inducing eddy current on the wedge surface with a certain current density (J_w). Since the pre-stressing strand and the wedge are composed of conductive material which is steel, the penetration depth (δ) of the eddy current is quite confined at the wedge surface.

$$\delta = \frac{1}{\sqrt{\pi f \mu \sigma}} \tag{7}$$

f is an alternating frequency (Hz) of H_p and, σ and μ mean an electric conductivity (S/m) and a magnetic permeability (H/m) of a material composing of a pre-stressing strand, respectively. Under the fact that a wedge consists of stainless steel ($\sigma \approx 1.45 \times 10^6$ S/m, $\mu \approx 1.26 \times 10^{-3}$ H/m), eddy current is confined to the wedge surface under the frequency of a few kHz so that δ becomes less than 1 mm. Note that, the current density of the generated eddy current on the wedge surface has closely related with its stress level according to the *piezo-resistive effects*.

(2) Measurement of V_c

Eddy current on the wedge surface in the step (1) produces H_s, which becomes combined with the existing H_p. According to the intensity of the H_s that is associated with J_w, the combined magnetic field of H_p and H_s passing through the pick-up coil is altered and results in the change of V_c.

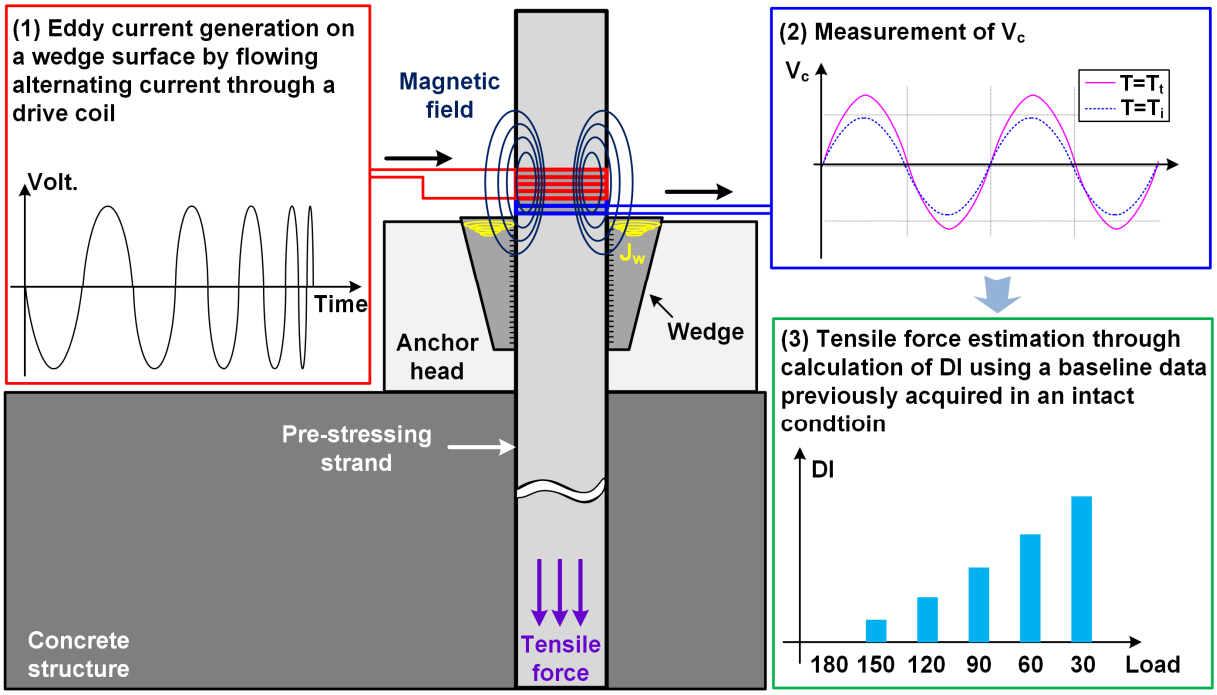

Fig. 3. Detailed working steps of the proposed EC-TFI

V_c acquired in the initial tensile force (T_i) means a baseline data to be used to estimate a target tensile force (T_t) which is relaxed from T_i. For instance, the variation of V_c under tensile force relaxation from T_i to T_t is shown in the step (2) of Fig. 3. For each tensile force condition which is needed to be estimated, the steps (1) and (2) are repeated and the level of relaxation is interpreted in the following step (3).

(3) Tensile force estimation through calculation of the defined damage index (DI):

In this step, a DI to detect a tensile force relaxation of the pre-stressing strand is defined using the measured V_c at both T_i and T_t:

$$DI_T = Var(V_c^{Target\_T}) - Var(V_c^{Initial\_T}) \quad (8)$$

$V_c^{Target\_T}$ and $V_c^{Intact\_T}$ are the measured V_c under T_i and T_t, respectively.

According to the *piezo-resistive effects* explained in Section 2.1, V_c is altered as the tensile force is decreased. DIs for different T_t, for example in this study 30 kN, 60 kN, 90 kN, 120 kN and 150 kN, are calculated using Eq. (8) and the magnitude of DI indicates the amount of the lost tensile force from T_i as shown in the step (3) of Fig. 3.

3. DEVELOPMENT OF EC-TFI SYSTEM

This section develops an EC-TFI system which is composed of an arbitrary waveform generator (AWG), a data acquisition (DAQ) system, an ECS and a control computer as shown in Fig. 4. Detailed operating procedure of the developed EC-TFI system is as follows.

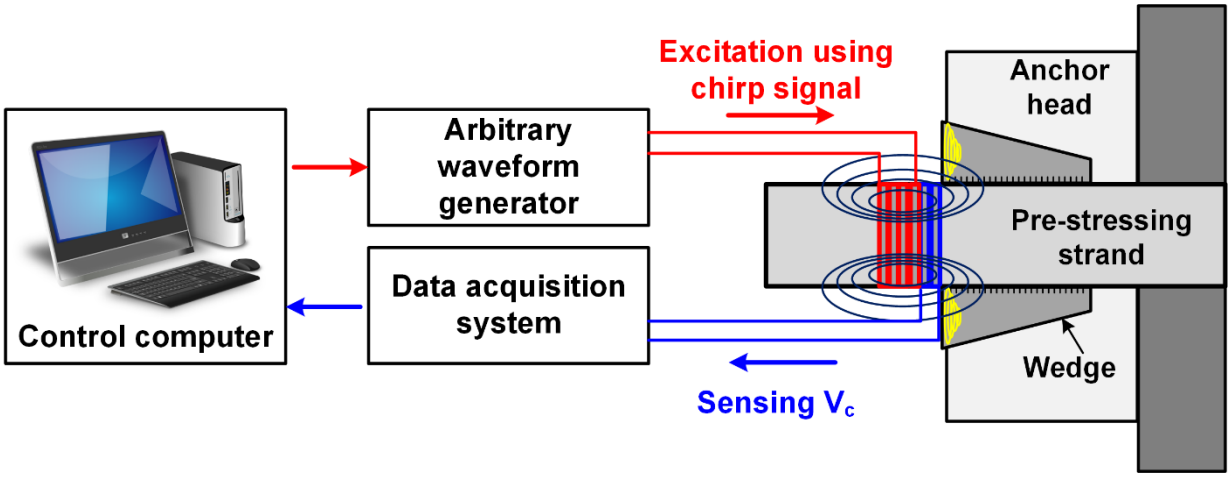

Fig. 4. Schematics of the developed EC-TFI system

First, let us suppose that a baseline data previously acquired in an initial condition is already stored in the control computer. When it is required to estimate tensile force of a pre-stressing strand, the control computer transfers a trigger signal to AWG and DAQ system in order to active the EC-TFI system. Then, AWG generates a chirp signal of

the pre-determined frequency range and amplitude, and directly transferred this signal to a drive coil. Alternating current through the drive coil induces corresponding H_p and in sequence, eddy current is produced on the wedge surface which is subjected to a certain compressed condition. Then, eddy current generates H_s, affecting the electromagnetic induction of the pick-up coil. V_c is acquired by the DAQ system with the pre-determined sampling frequency and, transferred and stored in the control computer. The acquired data is automatically processed and analysed using a proposed tensile force inspection algorithm coded by Matlab®, and essential functions for DAQ and synchronization between excitation and sensing process are controlled by LabVIEW™.

4. Experimental Validation

The performance of the developed EC-TFI system is experimentally validated using a 3.3 m long and Φ 15.2 mm pre-stressing strand and a specially designed universal tensile machine (UTM). As an initial condition, a tensile force of 180 kN is applied to the pre-stressing strand and V_c is measured for every step with 30 kN decrement from the initial tensile force of 180 kN. By calculating DI for each step, a force relaxation of the pre-stressing strand can be detected and estimated.

4.1 Experimental Setup

Fig. 5 shows experimental setup of the EC-TFI system. A 3.3 m long and Φ 15.2 mm pre-stressing strand is inserted on the UTM and, a load cell and a hydraulic actuator are located at right and left sides of the UTM, respectively. By considering a general design of a pre-stressing concrete girder, an initial tensile force is determined as 180 kN. Baseline data is acquired under 180 kN and then, tensile force is gradually decreased by 30 kN force step until it becomes 30 kN at the end.

In this experiment, the wedge produced by *Paul Company* is employed and its allowable tensile force is 2400 MPa. Cylinder-type ECS is specially designed and manufactured using a copper wire of Φ 0.08 mm in order to mount it through a pre-stressing strand. Diameter of the ECS is 16 mm which is slightly bigger than that of the strand, 15.2 mm.

ECS is composed of four layers of the copper wire in its radial direction and continuously stacked-up until its electric resistance becomes 20 Ω and 2.5 Ω for a drive and a pick-up coil, respectively. The detailed electric properties of the manufactured ECS are shown in Table. 1. The manufactured ECS is attached to the surface of the wedge at the side of the load cell.

AWG generates a chirp signal whose bandwidth is 10 kHz to 1,000 kHz, and its peak-to-peak voltage is 12 V. For measurements, DAQ time and sampling frequency are set as 0.1 second and 4 MHz, respectively.

4.2. Numerical Analysis to Observe Stress Distribution of a Wedge

A numerical simulation is performed using a finite element analysis software, COMSOL, to observe stress distribution of a wedge holding a pre-stressing strand. First, two-dimensional modeling is carried out to describe a pre-stressing strand. Although, in

fact, the pre-stressing strand is compose of seven steel wires, it is simplified into the form of a simple bar for convenience. Mechanical properties of a pre-stressing strand, a wedge and an anchor head such as young's modulus, Poisson's ratio and density are decided as shown in Table. 2. The frictional coefficients are supposed to two different contact surface: (1) between the strand and the wedge and (2) between the wedge and the anchor head. The former and the latter are set as 0.9 and 0.4, respectively. Note that, the frictional coefficient between the strand and the wedge is set as high, because a strong contact is expected through structural features of a teeth-shape at inner surface of the wedge biting the strand. And, bottom surface of the anchor head is subjected to the boundary condition of zero-displacement by a structure.

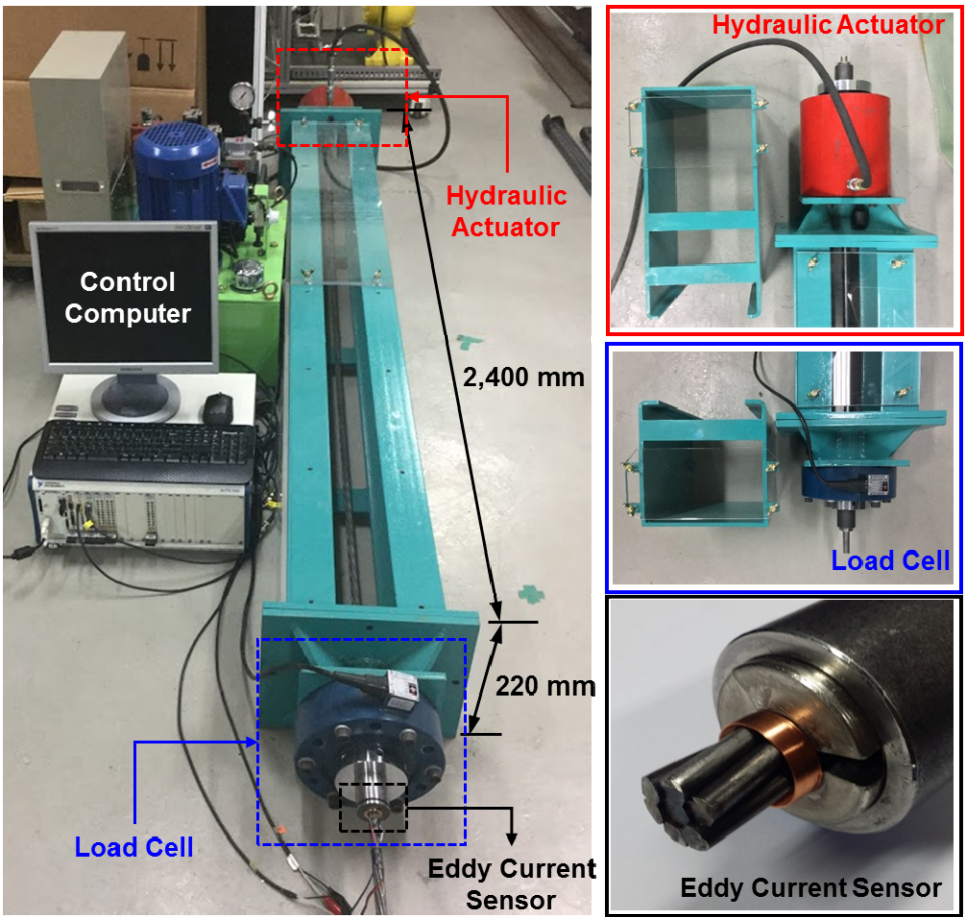

Fig. 5. Experimental setup of EC-TFI system using a cylinder-type ECS

Table. 1. Design parameters and electric properties of the manufactured ECS

	Drive coil	**Pick-up coil**
ECS Diameter (mm)	16	16
Wire diameter (mm)	0.08	0.08
Inductance (μH)	634.8	6.31
Resistance (Ω)	20	2.5

Table. 2. Mechanical properties of a pre-stressing strand, a wedge and an anchor head used for numerical analysis using COMSOL

	Pre-stressing Strand	Wedge	Anchor Head
Young's Modulus (GPa)	200	200	1000
Poisson's Ratio	0.33	0.33	0.35
Density (kg/m^3)	7850	7850	7850

When time *t* equals zero, the strand and the wedge are under a simple contact as we suppose in advance, and the wedge is located at 5 mm above the anchor head. In order to induce a stress to the wedge and the pre-stressing strand, a displacement is introduced to the strand so that the wedge is fitted into the anchor head and stress can be distributed to the wedge. As shown in Fig. 6, stress is not observed before displacement is introduced to the strand. As the strand moves downward, the contact pressure between structural components becomes strong. However, stress primarily arises through the pre-stressing strand. When displacement is reached at 5 mm, the wedge is exactly fitted to the anchor head and, the stress of the pre-stressing strand is redistributed to the wedge. In particular, large stress is mainly distributed at the wedge surface as we expected. If the displacement is applied more than 5 mm, for example 5.1 mm, structural deformation arises and stress concentration is more intensified at the wedge surface. Even though the simplified bar is used instead of three-dimensional model of real pre-stressing strand of seven steel wires, this results offer a good explanation and inference for stress redistribution of the pre-stressing strand to the wedge.

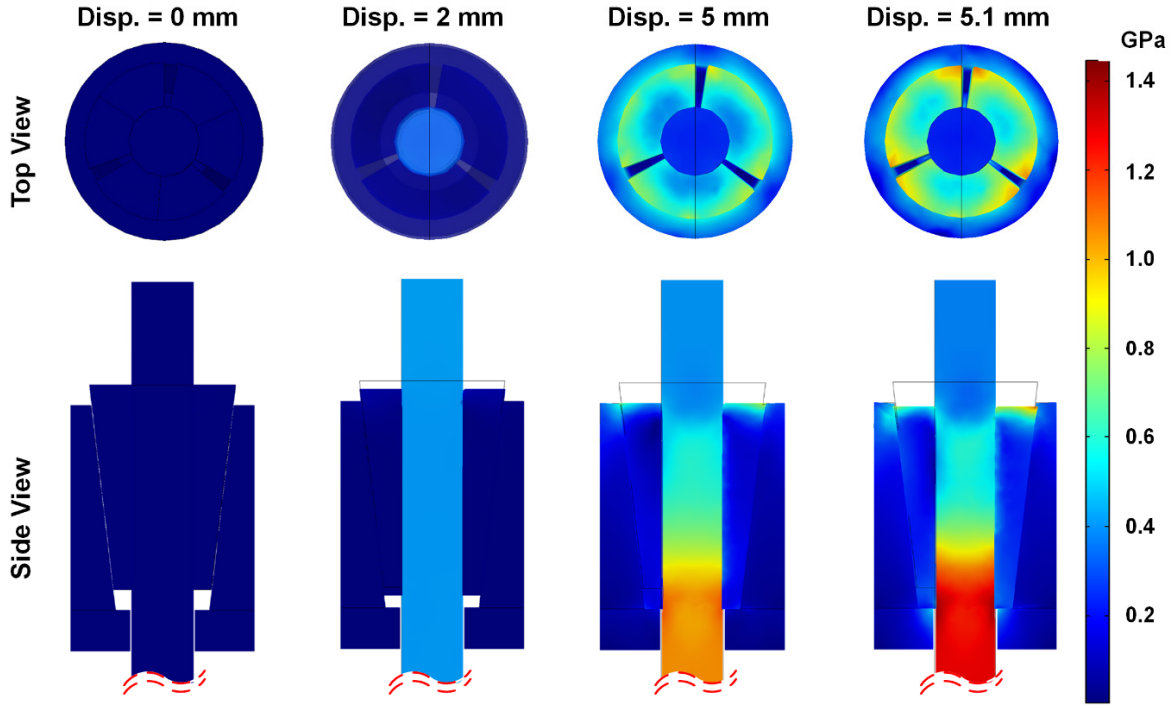

Fig. 6. Numerical simulation for stress distribution of a wedge holding a pre-stressing strand using finite element analysis

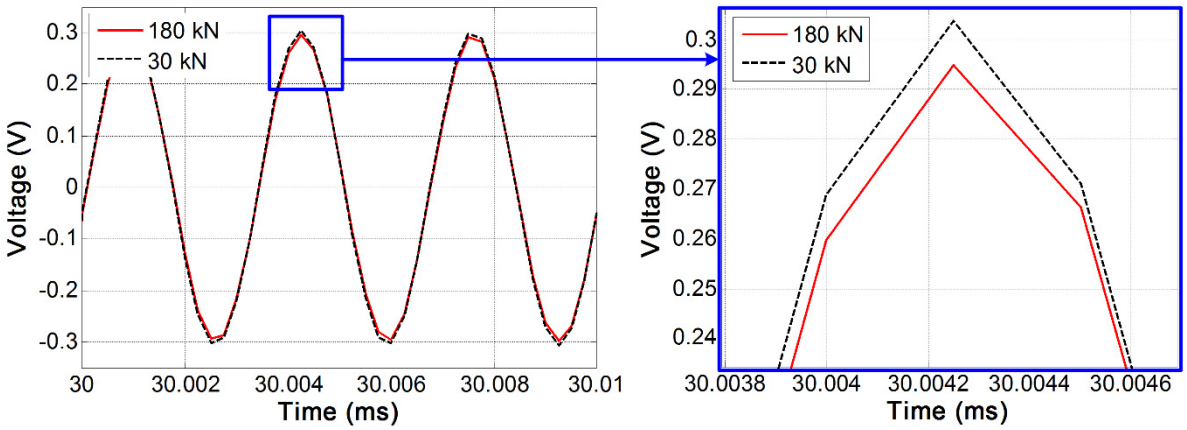

Fig. 7. Comparison the measured V_c's under 180 kN and 30 kN which is expressed using red-solid line and black-dotted line, respectively.

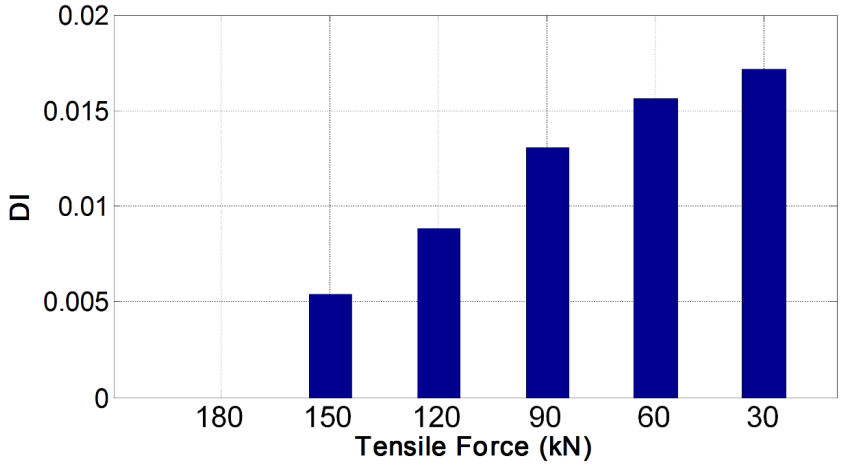

Fig. 8. DI comparison under 30 kN step-wise tensile force loss from an initial tensile force of 180 kN using a cylinder-type ECS

4.3. Experimental Results

First, V_c for each pre-determined tensile force step is measured. According to the *piezo-resistive effects*, eddy current density on the wedge surface, J_w, is altered by tensile force of the pre-stressing strand, which sequentially affects production of V_c. Fig. 7 shows the measured V_c for 180 kN and 30 kN which are expressed using red-solid line and black-dotted line, respectively. Because of variation of J_w and H_s by alteration of tensile force, the amplitude of the V_c for each tensile force condition shows clear difference.

In order to investigate and estimate the loss of the tensile force, DI is employed which is previously defined through Eq. (8) in Section 2. Calculated DI of each tensile

force is shown in Fig. 8. Since the measured V_c under 180 kN is considered as baseline data, i.e. $V_c^{Initial\_T}$, DI is turned out to be zero. On the other hand, as the tensile force of the pre-stressing strand is gradually relaxed, DI becomes larger. In particular, it is very promising that the relationship between DI and the amount of tensile force relaxation seems to be monotonic, meaning that EC-TFI system can be used in order to estimate how much force relaxation has been introduced from initial condition.

5. CONCLUSIONS

A new technique is proposed to detect tensile force relaxation of a pre-stressing strand through eddy current measurement having following advantages: (1) low cost, (2) low power consumption, (3) simple installation without disturbing existing construction process and (4) robustness sensor healthiness during construction. In this study, eddy current based tensile force inspection (EC-TFI) system is developed and its performance is experimentally validated using a 3.3 m long and Φ 15.2 mm pre-stressing strand which is tensioned by a specially designed universal tensile machine. As an initial condition, the pre-stressing strand was tensioned up to 180 kN and, an eddy current-induced voltage signal in a pick-up coil was acquired which is used as a baseline data. Through calculation of the proposed damage index (DI) for each tensile force with 30 kN decreasing step, tensile force relaxation of the pre-stressing strand was successfully estimated. A monotonic relationship between tensile force and the proposed DI was observed.

There are several issues to be considered for real applications in the future. First, the EC-TFI system should be carefully designed in a form of a compact and wireless sensor node, so that it is simply attached to a structure and carries out signal generation, DAQ and post-processing. In addition, a tensile force quantification algorithm is required, enabling to estimate a current tensile force, not simply to detect if it is relaxed or not.

ACKNOWLEDGEMENTS

This study is supported by a grant from Smart Civil Infrastructure Research Program (13SCIPA01) funded by Ministry of Land, Infrastructure and Transport (MOLIT) of Korea government

REFERENCES

Tadros, M.K. (2003), “NCHRP Report 496: Prestress losses in pretensioned high-strength concrete bridge girders”, Transportation Research Board, Washington, D.C.

Hewson, N.R. (2008), “Design of prestressed concrete bridges”, ICE Manual of Bridge Engineering, ICE Publishing, London, UK

Wang, G., Wang M.L., Zhao, Y., Chen, Y. and Sun, B. (2006), “Application of magnetoelastic stress sensors in large steel cables”, *Smart Struct. Syst.*, **2**(2), 155-169.

Duan Y.F., Zhang R., Zhao Y., Or S.W., Fan K.Q. and Tang Z.F. (2012), "Steel stress monitoring sensor based on elasto-magnetic effect and using magneto-electric laminated composite", *J. Appl. Phys.*, **111**, 07E516.

Bartoli, I., Salamone, S., Philips, R., Scalea, F.L. and Sikorsky, C.S. (2011) "Use of Interwire Ultrasonic Leakage to Quantify Loss of Prestress in Multiwire Tendons", *J. Eng. Mech-ASCE*, **137**, 324-333

Kim, J.M., Kim H.W., Park, Y.H., Yang I.H. and Kim, Y.S. (2012), "FBG Sensors Encapsulated into 7-Wire Steel Strand for Tension Monitoring of a Prestressing Tendon", *Adv. Struct. Eng.*, **15**(6), 907-917.

Lan, C., Zhou, Z. and Ou, J. (2014), "Monitoring of structural prestress loss in RC beams by inner distributed Brillouin and fiber Bragg grating sensors on a single optical fiber", *Struct Control Hlth*., **21**(3), 317-330

Schoenekess, H.C., Ricken, W. and Becker, W.J. (2007), "Method to Determine Tensile Stress Alterations in Prestressing Steel Strands by Means of an Eddy-Current Technique", *IEEE Sen. J.*, **7**(8), 1200-1205

Jackson, J.D. (1998), Classical Electrodynamics 3rd Edition, John Wiley & Sons, New York, NY